Hexagonally Reconstructed Islands and Anisotropic Diffusion for Au/Au(100)

Miki Nomura and Xiao-Qian Wang

Department of Physics and Center for Theoretical Studies of Physical Systems, Clark Atlanta University, 223 James P. Brawley Drive, Atlanta, Georgia 30314

(Received 27 January 1998)

The homoepitaxial island growth on hexagonally reconstructed Au(100) is studied using molecular dynamics based on a well-tested many-atom interatomic potential. Our study reveals that the stable islands of rectangular shape are hexagonally reconstructed in conformity with the patterns of the reconstructed Au(100) surface and suggests the "magic" stable width for the reconstructed islands in agreement with experimental observations. Furthermore, our results on the adatom diffusion indicate that the experimentally observed strong anisotropic effect is attributed to the long-range exchange diffusion. [S0031-9007(98)07233-0]

PACS numbers: 68.35.Fx, 68.10.Jy, 68.35.Bs, 68.55.–a

Surface adatoms and small cluster diffusion on metal clusters have been the subject of recent experimental and simulational attention due to their important role played in controlling the formation of surface layers, thin film growth, and catalysis. The nucleation and growth of Au islands on the reconstructed Au(100) are both intrinsically interesting and technologically important. It is expected that for the island growth, surface morphology depends strongly on the reconstructed substrate. Recently, Günther and co-workers [1] carried out a scanning-tunneling microscope (STM) study of the nucleation and growth of Au islands on the hexagonally reconstructed Au(100) surface. It was shown that the reconstructed substrate yields strong anisotropic effects, specifically the rectangular shape of the island (island shape anisotropy) and strongly anisotropic diffusion. The latter was deduced from the rate equation analysis of the experimental flux and temperature dependence of the island density. Two typical sizes of the islands, namely, (i) islands of widths of 30 Å and lengths ranging from 100 to 150 Å at high deposition flux rate and (ii) islands of widths of less than 80 Å and lengths around 700 Å at low deposition flux rate, were reported.

In spite of this intriguing picture, there has remained a paucity of theoretical studies on the island growth and anisotropic diffusions for Au/Au(100). A clear understanding of the origin of anisotropic effects has been hindered by the lack of quantitative theoretical calculations. Recently, Bonig, Liu, and Metiu [2] employed the effective-medium theory to investigate the diffusion of adatoms for a m-atom-wide (1×5) reconstructed island on top of unreconstructed underneath. Their calculation indicates that kinetics favors $m = 6$, in that the adatom diffusion along the long side of such a reconstructed island is much faster than $m \neq 6$. However, due to the limitation of the employed interatomic potential (not capable of predicting the reconstructed surface), their interpretation of experiments needs to be reexamined with more realistic models.

Inspired by the experimental results, we have carried out a large-scale molecular-dynamics (MD) simulation study of the island growth and anisotropic diffusion on Au/Au(100). Using a well-tested many-atom potential of gold constructed by Ercolessi, Tosatti, and Parrinello [3], our simulation study reveals that the optimal island is "quantized" in concord to the "magic" size of $7, 13, \ldots$ $(6n + 1$, where n is an integer) reconstructed rows. The formation of a hexagonally reconstructed island in conformity with the pattern of the reconstructed Au(100) surface is energetically favored. Contrary to the proposed hopping mechanism for adatom diffusion [2], our calculation reveals that the long-range exchange effect plays a predominant role in the anisotropic diffusion and the growth of hexagonally reconstructed islands.

The semiempirical many-body "glue model" [3] belongs to the same class as the embedded-atom method [4] and "pair-functional" models [5]. The glue potential for gold has been well tested and is known to provide good results for diverse surface properties. Specifically, the model is capable of explaining the structure and phases of the reconstructed Au(100) surface. It is worthwhile to mention that the simulation study of $(M \times 5)$ reconstruction configuration (i.e., $M + 1$ first-layer atoms on top of M second-layer atoms along [011], in addition to the 6-onto-5 registry along $[01\bar{1}]$), reveals that the energies are very close for the range $20 < M < 35$, with a surface energy difference of 0.1 meV/Å^2 [3,6].

In carrying out our analysis, we have performed intensive molecular-dynamics simulations, with in-plane periodic boundary conditions, on 16-layer slab systems consisting of $(2–5) \times 10^4$ atoms. The experimentally observed (28×5) structure [7,8] is used for the surface throughout this study. The structure can be characterized by edge dislocations along [011] and $[01\bar{1}]$, respectively, with the dislocation lines corresponding to the corrugated regions in connection with the excessive stress. It is worth noting that the corrugated lines can be identified as parallel stripes observed in STM experiments.

Magic island width.—To study the optimal rectangular island structure, we have investigated three characteristic configurations, namely, (i) a (1×1) island of square lattice structure on a reconstructed (28×5) surface, (ii) a hexagonally reconstructed (28×5) island on the (28×5) reconstructed surface, and (iii) a reconstructed (28×5) island on top of a (1×1) underneath substrate, while the surface structure remains reconstructed. The change of surface energy due to the existence of an island is

$$\Delta E_S = (E_{\text{tot}} - NE_{\text{coh}})/A - E_S\,, \tag{1}$$

where E_{tot} is the total energy of the system, E_{coh} the cohesive energy, N the number of atoms of the system, A the total area of the surface, and E_S the surface energy without the island.

As seen from Table I, the reconstructed island on a unreconstructed substrate stands for the most favorable configuration in energy. Our calculation is the first direct theoretical confirmation of the experimental implication of reconstructed island being the optimal structure.

There exist a large number of configurations for the reconstructed island. They can be classified according to the number of rows (width), smooth or steep edges, the length of the island, and finally, the location of the island with respect to the surface structure. As can be observed from Tables I and II, the quantized islands with $6n + 1$ rows (n an integer) and smooth edge [$(28 \times 5)_{6n+1}/(1 \times 1)$ hereafter] are energetically preferred, as the unquantized reconstructed islands (including the $(1 \times 5)_6/(1 \times 1)$ [2]) have surface energy ~ 2–4 meV/Å^2. Figures 1 and 2 show the side and top views of an optimized $(28 \times 5)_{13}/(1 \times 1)$ island structure.

It is worth noting that the $(28 \times 5)_{6n+1}/(1 \times 1)$ configuration can arise from a transformation from the $(1 \times 1)_{5n}/(28 \times 5)$ through a release of the stress associated with contracted reconstruction surface, in that the $n + 1$ corrugated rows pop up as the edge of the island. As a result of such a transformation, the island is reconstructed in conformity of the (28×5) pattern, while the underneath layer is recovered back to the (1×1) square structure. Illustrated in Fig. 3 is such a transformation process for $n = 2$.

This scenario for the formation of the hexagonally reconstructed island has been confirmed through MD simulations. The corrugated dislocation lines incorporate themselves into the island structure, forming a hexagonally reconstructed island with n new corrugated dislocation lines. After the completion of this work, we became aware of the fact that experimental STM study observed exactly the same structure, a quantized island in width and smooth edge, with n parallel stripes on the island structure [9]. Specifically, the two types of islands (under high and low deposition rates [1]) correspond to $n = 2$ (30 Å) and $n = 5, 6$ (80 Å), respectively.

Size of the islands.—The experimental observation on the dependence of island size on the deposition flux rate can be qualitatively interpreted from our simulation study. Shown in Table II are the changes of surface energies and the corresponding step energies with respect to different magic width. As seen from Table II, the energy difference for different width is small, while from an energetic point of view the larger islands (with smaller step energies) are preferred.

To shed light on the mechanism of island formation, we have carried out intensive MD simulations of randomly deposited adatoms at finite temperatures for about 20 psec. It has been observed that after fast annealing of initial configurations, for low coverages ($\leq$10% monolayer), almost all the adatoms sink into the already compressed reconstructed surfaces, with a fraction of adatoms diffusing into the second layer. With the increase of the coverage, the reconstructed island/surface layer can accommodate up to 4.5% monolayer (ML) adatoms, and the second layer of square symmetry can accommodate up to 5% ML adatoms; the remaining adatoms stay on top of the highly constrained surface layers, with small islands of the size of about ten adatoms being formed. The "sunk-in" phenomenon is largely connected to the fact that the energy difference among the $(M \times 5)$ reconstructed surface/island configurations is very small, as can be seen from Table III for several reconstructed islands of the same width. Roughly speaking, the (44×5), (28×5), and (20×5) reconstructed islands correspond to adding one, two, and three columns of adatoms to the (1×5) island, respectively.

The above described "skin-deep" mechanism for island growth offers an explanation of the experimental observation that the growth is two dimensional in that the adatoms falling on top of the island readily sink in. On the other hand, the fast-annealed structure is not stable at finite temperature against thermal activations. Indeed, our MD simulation at finite temperatures, e.g., at 400 K, reveals that the overly constrained layers move like waves. The

TABLE I. The change in surface energy for three prototype island structures.

Island	ΔE_S (meV/Å^2)
$(1 \times 1)_{10}/(28 \times 5)$	8.01
$(28 \times 5)_{13}/(1 \times 1)$	1.35
$(28 \times 5)_{13}/(28 \times 5)$	3.99

TABLE II. The change in surface energy for reconstructed islands with different width ΔE_S, and the corresponding width step energy (ΔE_S divided by the length of the island width).

Island	ΔE_S (meV/Å^2)	E_{step} (10^{-2} meV/Å^3)
$(28 \times 5)_7/(1 \times 1)$	1.21	4.21
$(28 \times 5)_{13}/(1 \times 1)$	1.35	2.34
$(28 \times 5)_{19}/(1 \times 1)$	1.59	1.84
$(28 \times 5)_\infty/(1 \times 1)$	0.71	0

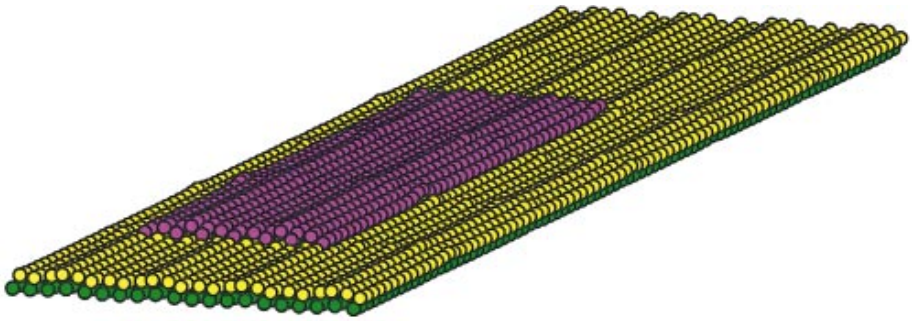

FIG. 1(color). The optimized configuration of a reconstructed island (violet atoms) on top of the (28 × 5) layer (yellow atoms). Also shown is the second layer (green atoms) of the slab. Note the corrugated rows of the island sit in between the corrugated rows of the (28 × 5) reconstructed surface.

small islands formed on the surface tend to form larger ones through two mechanisms. One involves the forming of a reconstructed island via the transformation discussed above, and the other involves the reduction of the effect of the island edge. This implies that the islands tend to reconstruct and then form larger ones given sufficient time for equilibrium. In practice, the island formation with different deposition flux rates is a kinematic process. With high deposition flux rate, the predominant mechanism is the island reconstruction so that the small islands are formed; while for low deposition flux rate, the second mechanism takes into account and thus larger islands are formed. Although a MD simulation of the process at the experimental time scale is not feasible, the experimentally observed island size dependence on the deposition flux rate may be qualitatively understood along the above-described lines.

Anisotropic diffusion.—The rate equation study [1] of the experimental flux and temperature dependence of the island density suggests that diffusion of adatoms along and perpendicular to the island edge is strongly anisotropic. We have studied the single adatom diffusion along the edges of reconstructed island. The migration energy is found about 0.6 eV along the edge of the reconstructed row, and about 1.4 eV along the edge perpendicular to the reconstruction row. While the calculation supports the anisotropic diffusion, the calculated migration barrier is much larger than that suggested by the rate equation study. The suggested [1,2] diffusions of dimers and trimers are not favored in the present model as they readily break apart.

The above study on the diffusion assumes conventional pathways of hopping diffusion [10]. For single adatom on the reconstructed islands and surfaces, the stable site corresponds to the one right on top of the "second layer" atoms that are of a square symmetry. The diffusion paths are thus primarily straight lines, similar to those for Ag(100) [11]. However, a striking distinct feature is that a large portion of such stable sites, mostly those away from the corrugated regions, sink into the reconstructed island/surface. This contradicts the intuitive notion that the stable site of adatoms is floating on top of the island/surface. Diffusion migration energies along and perpendicular to the reconstruction rows are strongly site dependent. As a result of the existence of this kind of stable sunk-in adatom sites, long-range diffusion path ($>$6 Å) becomes possible, with the migration energy as low as 0.2 eV along the reconstruction rows. One should be cautious to compare this with the estimated value extracted from rate equation study of the experimental data, since the cooperative effect of other adatoms is no longer negligible, and the energy barriers are not sufficient to conclude about the contribution of hopping and exchange mechanism to the total diffusion [12].

Recently, Yu and Scheffler [13] predicted that exchange diffusion should occur on Au(100) based on a density-functional theory study. While the prediction focuses on the local exchange mechanism, our MD simulation study

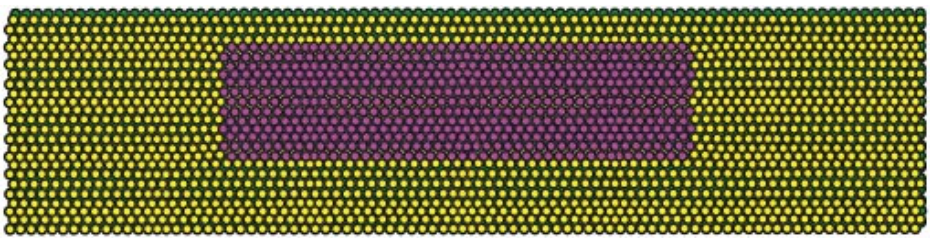

FIG. 2(color). The top view of the optimized configuration of a reconstructed island (violet atoms), the (28 × 5) layer (yellow atoms), and the second layer (green atoms) of the slab.

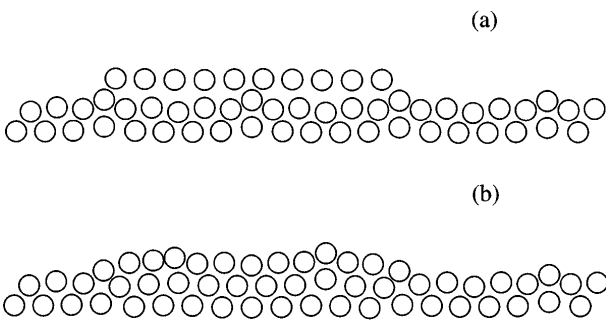

FIG. 3. Side view of (a) unreconstructed island on top of a reconstructed (28 × 5) surface, and (b) a hexagonally reconstructed island on top of a unreconstructed underneath substrate. The transformation from (a) to (b) involves the "pop up" of the corrugated rows associated with the reconstructed (28 × 5) layer, together with a lateral displacement of the reconstruction rows. Notice that the corrugated rows in both the reconstructed island and the (28 × 5) surface can be directly observed by STM experiments.

TABLE III. The change in surface energy for reconstructed island structures with different contraction in length.

Island	ΔE_S (meV/Å^2)
$(20 \times 5)_{13}/(1 \times 1)$	1.62
$(28 \times 5)_{13}/(1 \times 1)$	1.35
$(44 \times 5)_{13}/(1 \times 1)$	1.46
$(1 \times 5)_{13}/(1 \times 1)$	1.86

with realistic surface reconstruction structure suggests a long-range exchange diffusion process. In this process, the adatoms first sink into the reconstructed island or surface, resulting in local distortions of the hexagonal order and excessive tensile strain. The excessive strain can be released via cooperative motions of atoms involving in reconstructed rows and transformation between the surface/island and underneath layers. Our long-time MD simulation study at finite temperatures, e.g., at 400 K, reveals that such a diffusion process is clearly observable. Such a diffusion process can be characterized as "long-range exchange," different from the traditional hopping process considered in previous theories [2].

In summary, we have carried out an intensive MD simulation study of the island growth and diffusion mechanism of gold atoms on the hexagonally reconstructed Au(100) surface. Our study shows that the hexagonally reconstructed islands with magic width of $6n + 1$ rows and smooth edges are the energetically favorable configurations, in agreement with the experimental observations. Furthermore, our calculation suggests that the anisotropic diffusion mechanism can be attributed to the cooperative motion of adatoms associated with the release of local stress, rather than the usual adatoms hopping mechanism. Moreover, the exchange diffusion can be long ranged, not limited to the short-range exchange diffusions described in other theories [13].

This work was supported by the National Science Foundation under Grant No. HRD9450386, Air Force Office of Scientific Research under Grant No. F49620-96-1-0211, and Army Research Office under Grant No. DAAH04-95-1-0651.

[1] S. Günther, E. Kopatzki, M. C. Bartelt, J. W. Evans, and R. J. Behm, Phys. Rev. Lett. **73**, 553 (1994).
[2] L. Bonig, S. Liu, and H. Metiu, Surf. Sci. **365**, 87 (1996).
[3] F. Ercolessi, E. Tosatti, and M. Parrinello, Phys. Rev. Lett. **57**, 719 (1986); Surf. Sci. **177**, 314 (1986).
[4] S. M. Foiles and M. S. Daw, Phys. Rev. B **38**, 12 643 (1988); S. M. Foiles, M. I. Baskes, and M. S. Daw, Phys. Rev. B **33**, 7983 (1986).
[5] A. E. Carlsson, Solid State Phys. **43**, 1 (1990).
[6] X. Q. Wang, Phys. Rev. Lett. **67**, 3547 (1991).
[7] S. G. J. Mochrie, D. M. Zehner, B. M. Ocko, and Doon Gibbs, Phys. Rev. Lett. **64**, 2925 (1990); B. M. Ocko, Doon Gibbs, D. M. Zehner, and S. G. J. Mochrie, Phys. Rev. B **44**, 6429 (1991), and references therein.
[8] D. L. Abernathy, D. Gibbs, G. Grübel, K. G. Huang, S. G. J. Mochrie, A. R. Sandy, and D. M. Zehner, Surf. Sci. **283**, 260 (1993).
[9] S. Günther and M. C. Bartelt (private communcation).
[10] C. L. Liu, J. M. Cohen, J. B. Adams, and A. F. Voter, Surf. Sci. **253**, 334 (1991).
[11] Byung Deok Yu and Matthias Scheffler, Phys. Rev. Lett. **77**, 1095 (1996); Phys. Rev. B **55**, 13 916 (1997).
[12] N. I. Papanicolaou, G. A. Evangelakis, and G. C. Kallinteris, Comput. Mater. Sci. **10**, 105 (1998).
[13] Byung Deok Yu and Matthias Scheffler, Phys. Rev. B **56**, R15 569 (1997).